872 *Macromolecules* **2011**, *44*, 872–877
DOI: 10.1021/ma1024126

Macromolecules
ARTICLE

Low-Band-Gap Polymers That Utilize Quinoid Resonance Structure Stabilization by Thienothiophene: Fine-Tuning of HOMO Level

Nabil Kleinhenz,[†] Liqiang Yang,[‡] Huaxing Zhou,[†] Samuel C. Price,[†] and Wei You*[,†,‡]

[†]*Department of Chemistry, University of North Carolina at Chapel Hill, Chapel Hill, North Carolina 27599-3290, United States, and* [‡]*Curriculum in Applied Sciences and Engineering, University of North Carolina at Chapel Hill, Chapel Hill, North Carolina 27599-3287, United States*

Received October 22, 2010; Revised Manuscript Received December 29, 2010

ABSTRACT: Compared with the dominant donor−acceptor approach to construct low-band-gap polymers, the quinoid strategy has been much less explored. However, a new series of polymers based on a prequinoid structure, thieno[3,4-*b*]thiophene (TT), and a comonomer, benzo[1,2-*b*:4,5-*b*′]dithiophene (BnDT), have recently achieved over 7% power conversion efficiency in bulk heterojunction (BHJ) polymer solar cells (PSC). In order to further explore the utility of the thienothiophene (TT), we studied a library of six polymers by varying the electronic properties of the comonomers (NDT, naphtho[2,1-*b*:3,4-*b*′]dithiophene, QDT, dithieno-[3,2-*f*:2′,3′-*h*]quinoxaline, and BnDT) and those of the thienothiophene (TT and fluorinated TT (FTT)). It was discovered that the thienothiophene unit predominantly decides the low-band-gap characteristic of these polymers; however, the highest occupied molecular orbital (HOMO) energy level of these polymers can be tuned, depending upon the electronic properties of the comonomer and the substitution of fluorine on TT. Therefore, the open-circuit voltage of related BHJ devices changes accordingly. However, all observed short circuit currents were low, which limited the overall efficiency of all devices to less than 1%. Plausible reasons for such low currents include low molecular weight, unoptimized side chains, and low hole mobilities. These results indicate that materials optimization to achieve high efficiency polymer solar cells is a convoluted process; side chain length (and shape) and molecular weight, in addition to band gap and energy levels, all need to be carefully evaluated.

Introduction

In the quest to develop cost-effective renewable energy, polymer solar cells (PSC), specifically bulk heterojunction solar cells (BHJ), which usually employ electron-donating polymers and fullerene-based acceptors, have stood out as an attractive alternative to prohibitively costly silicon-based inorganic solar cells.[1−3] Significant progresses have been made in designing semiconducting polymers with low band gaps (maximizing the light absorption and the short-circuit current, J_{sc}) and low highest occupied molecular orbital (HOMO) energy levels (maximizing the open-circuit voltage, V_{oc}), with efficiencies of over 7% achieved recently in a number of reports.[4,5]

Two different approaches are usually employed in developing new polymers of narrow band gap for BHJ solar cells. The first and most common one is the donor−acceptor (D−A) approach to covalently link an electron-donating moiety and an electron-accepting moiety as the repeating unit of the D−A copolymer.[6,7] The band gap of such a polymer is narrowed through the formation of a quinoid resonance structure via intramolecular charge transfer (ICT).[8,9] The unique feature of this approach is that the HOMO level of these D−A copolymers is predominantly determined by the donor moiety, and the lowest unoccupied molecular orbital (LUMO) almost exclusively resides on the acceptor moiety.[10−12] This allows a largely independent control of the HOMO energy level (affecting V_{oc}) and the band gap (deciding J_{sc}). The second and much less explored approach to lowering the band gap is through the quinoid resonance structure stabilization.[13−16] Typically, two aromatic units are fused in a particular geometry to take advantage of the larger value of resonance energy of the first aromatic unit (e.g., benzene, 1.56 eV) over the second unit (e.g., thiophene, 1.26 eV), so that the second aromatic unit (e.g., thiophene) tends to dearomatize to adopt a quinoid structure. Since the quinoid resonance form is lower in energy than the aromatic form, stabilizing the quinoid form will effectively reduce the band gap of related conjugated polymers. Advantages of this quinoid approach include the complete elimination of charged species in the resonance structure of the conjugated backbone (Figure 1) and continuous π orbitals, both of which could potentially improve the hole mobility due to fewer instances of charge trapping.[17] Although the quinoid approach is far less explored than the D−A approach, a series of copolymers of alternating benzo[1,2-*b*:4,5-*b*′]dithiophene (BnDT) and thieno-[3,4-*b*]thiophene (TT) units (or monofluorinated TT unit, FTT), i.e., PTB series, have set record power conversion efficiencies of greater than 7% in polymer solar cells.[4,5] This significant achievement testifies to the viability of the quinoid approach in developing low-band-gap materials with high efficiency. In other studies, however, this quinoid approach has been far less successful.[18] In addition, the quinoid approach does have one disadvantage: it is more difficult to independently control the HOMO/LUMO energy levels due to the lack of a designated electron donor and acceptor. This implies that low-band-gap polymers incorporating quinoid structures would not necessarily own a low HOMO energy level. In contrast, one could achieve both a low band gap and a low HOMO level from the D−A approach.[19]

Even with the success of the PTB series, two outstanding questions still remain. The first one is whether the high performance of the PTB series is an exception or whether the TT/FTT unit can be employed to yield highly efficient polymers with fused aromatic

*To whom all correspondence should be addressed. E-mail: wyou@email.unc.edu.

 Published on Web 01/21/2011

comonomers other than BnDT (Figure 2). The second question is whether or not one can control the HOMO and LUMO energy levels of the quinoid-type copolymer by changing the electron-donating ability of the comonomer to the TT unit. If the energy levels of quinoid-type resonance structures could be fine-tuned by varying the electron-donating ability of the comonomer, the quinoid approach would offer control over both the current (via the band gap) and the voltage (via the HOMO level) of related BHJ solar cells, thus making it even more attractive as an alternative to the D−A approach.

As part of our attempt to answer these questions, we conducted a detailed investigation of a small library of new polymers incorporating the TT or FTT structural unit with two alternative fused aromatic comonomers, naphtho[2,1-*b*:3,4-*b*′]dithiophene (NDT) and dithieno[3,2-*f*:2′,3′-*h*]quinoxaline (QDT), which have been proven to have different electron-donating abilities (Figure 2).[20] For comparative purposes, an additional pair of polymers consisting of BnDT and TT/FTT monomers was also synthesized for the control study in which high power conversion efficiencies were expected. Indeed, all polymers show low-band-gap character. Furthermore, the HOMO energy level varies depending upon the electronic properties of the comonomer (NDT, QDT, or BnDT), which directly impacts the observed open-circuit voltage (V_{oc}). However, all obtained short-circuit currents (J_{sc}) are small, which led to overall efficiencies below 1%.

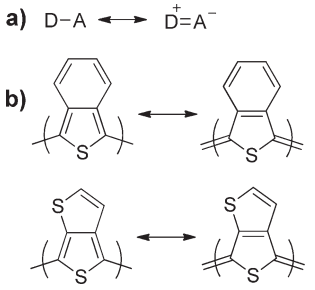

Figure 1. Donor−acceptor vs quinoid approach. (a) Donor−acceptor type polymer with low band gap due to increased double-bond character between monomers. (b) Example of quinoid resonance stabilized polymers, showing formation of aromatic benzene or thiophene unit which stabilizes quinoid resonance structure.

Results and Discussion

Monomer and Polymer Synthesis. In order to use Stille coupling polymerization to construct the small library of polymers, two thienothiophene units were synthesized and dibrominated according to literature procedures to offer the prequinoid monomers: 2-ethylhexyl 4,6-dibromothieno[3,4-*b*]-thiophene-2-carboxylate (TT)[21] and octyl 4,6-dibromo-3-fluorothieno[3,4-*b*]thiophene-2-carboxylate (FTT).[22] The other three monomers, naphtho[2,1-*b*:3,4-*b*′]dithiophene (NDT), dithieno[3,2-*f*:2′,3′-*h*]quinoxaline (QDT), and 4,8-bis(3-butylnonyl)benzo[1,2-*b*:4,5-*b*′]dithiophene (BnDT), were synthesized and distannylated according to literature procedures.[23−25] A small library of six polymers was thus prepared for further study (Scheme 1).

All polymers were carefully purified. For polymers made according to condition 1 in Scheme 1, the reaction mixture after each polymerization was precipitated into methanol to offer the crude polymer, which was collected and further purified by Soxhlet extractions with methanol and ethyl acetate successively to remove byproducts and oligomers. Finally, the polymer was Soxhlet extracted with hexane, THF, or chloroform and recollected by precipitation into methanol and dried under vacuum to yield dark blue solids. For PBnDT-TT, synthesized according to condition 2 in Scheme 1, the reaction mixture was precipitated into methanol, and the resulting crude polymer was dissolved in $CHCl_3$, filtered through Celite to remove the metal catalyst, and then precipitated into ethyl acetate and dried under reduced pressure to yield a dark blue solid. The yields and molecular weights of the polymers are listed in Table 1. Molecular weights were determined by gel permeation chromatography (GPC) in THF by referring to polystyrene standards. The high molecular weight of the PBnDT-TT and PBnDT-FTT polymers can be attributed to a better solubility in the polymerization solvent due to the longer C13 side chains on the BnDT unit compared to C8 side chains on the NDT and QDT unit.

Optical and Electrochemical Properties. The solution and film absorption spectra of all six polymers are shown in Figure 3. Generally, all six polymers are low-band-gap materials, with band gaps as small as 1.4 eV in the case of PNDT-TT (Table 2). It appears that the thienothiophene unit predominantly decides the band gap of these six polymers; changing

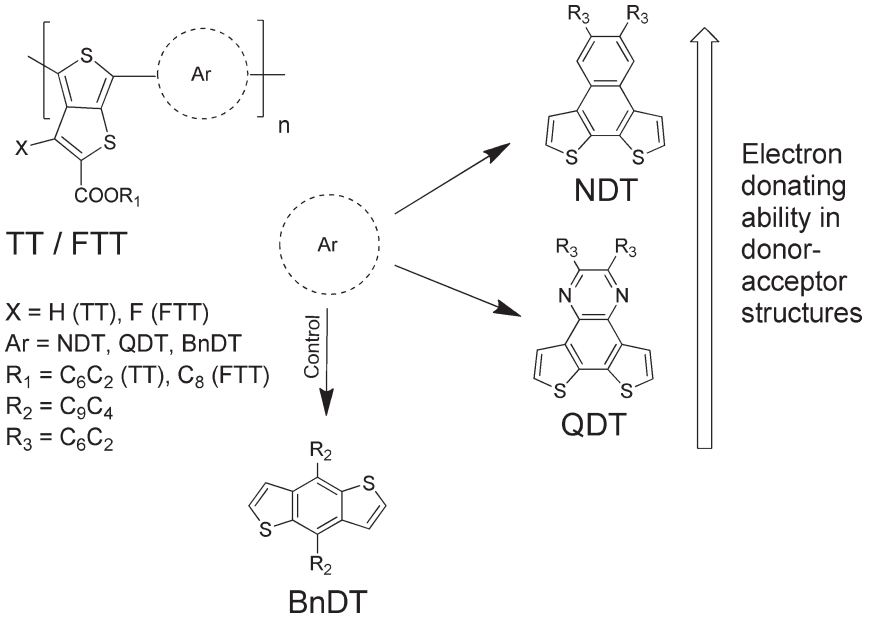

Figure 2. Studied library of polymers incorporating the thienothiophene (TT or FTT).

Scheme 1. Synthesis of Polymers via Palladium-Catalyzed Coupling Reactions[a]

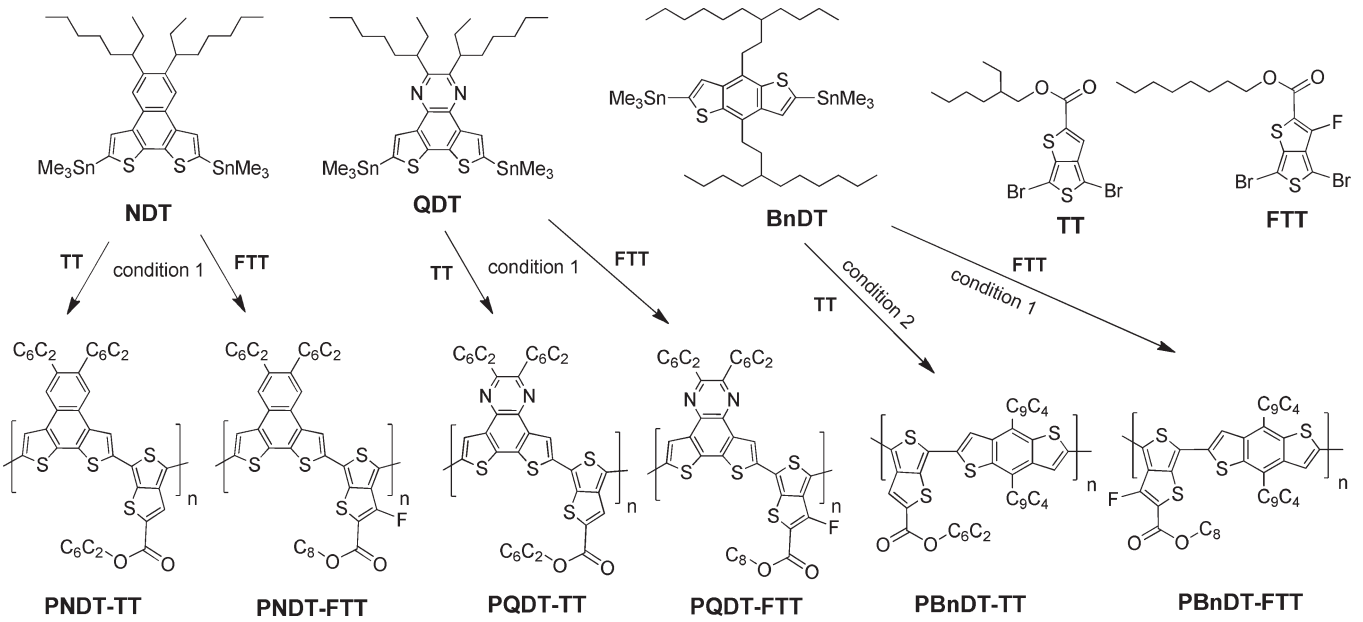

[a] Conditions: (1) *o*-dichlorobenzene, $Pd_2(dba)_3$/P(*o*-tol)$_3$ = 1:8, 150 °C, microwave 300 W, 20 min; (2) toluene, $Pd_2(dba)_3$/P(*o*-tol)$_3$ = 1:8, reflux 24 h, no Soxhlet extraction (just filtered through Celite) for condition 2.

Table 1. Polymerization Results for Polymers

polymer	yield [%]	M_n [kg/mol][a]	M_w [kg/mol][a]	PDI
PNDT-TT	51	19.9	51.0	2.56
PNDT-FTT	58	14.0	24.6	1.76
PQDT-TT	29	13.2	26.0	1.97
PQDT-FTT	68	12.1	23.2	1.91
PBnDT-TT	64	42.7	80.1	1.88
PBnDT-FTT	23	41.9	61.6	1.47

[a] Determined by GPC in THF using polystyrene standards.

the structure of the other comonomers (e.g., NDT, QDT or BnDT) or adding fluorine onto thienothiophene (from TT to FTT) makes very little impact to the observed optical band gap.

However, varying the structure of the comonomer (NDT, QDT, or BnDT) does affect the energy levels of the polymers based on the TT unit, as does the switching from TT to FTT (Table 2). First, the HOMO energy level increases with the electron-donating ability of the comonomer to the thienothiophene. For example, since the QDT in PQDT-TT is less electron donating than the NDT in PNDT-TT,[23] the HOMO in PQDT-TT is ~0.3 eV lower than that in PNDT-TT (−4.99 eV vs −4.70 eV). This demonstrates some degree of control of at least the HOMO level of the polymers with an identical prequinoid structure (TT or FTT).

It is interesting to notice that the HOMO energy level of PBnDT-TT in this study is the lowest among the three TT based copolymers even though BnDT appears to be more electron donating compared with QDT. Two plausible reasons account for this observation. First, the noticeably longer side chains with bigger branches (C9C4) on the BnDT would interfere with the $\pi-\pi$ stacking between polymer chains, leading to a decrease in the HOMO level.[26] For example, a HOMO energy level of −5.04 eV was observed when straight C8 chains were anchored on the BnDT,[22] in contrast to −5.12 eV in C9,4-PBnDT-TT of this study. Second, the structural configuration/geometry of BnDT is different from that of NDT or QDT. In BnDT, the two flanking thiophene units are attached to the center benzene in an opposite orientation (with regard to the sulfur) in a linear fashion, adopting a C_{2h} symmetry, while the same thiophene

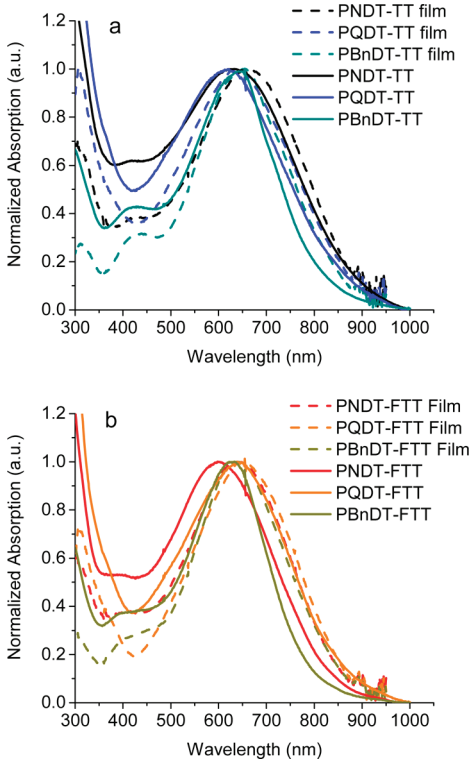

Figure 3. UV−vis spectra of all polymers: (a) PNDT-TT, PQDT-TT, and PBnDT-TT polymers in chlorobenzene solution (solid line) and in solid film (dash line) and (b) PNDT-FTT, PQDT-FTT, and PBnDT-FTT polymers in chlorobenzene solution (solid line) and in solid film (dashed line).

units are fused to the center benzene with a bent geometry (C_{2v} symmetry) in the case of NDT or QDT. These differences further explain the seemingly "unusual" behavior of PBnDT-TT.[27,28]

On the other hand, substituting the only remaining aromatic hydrogen of the thienothiophene with a strong electron-withdrawing fluorine (i.e., turning TT into FTT) unanimously

Table 2. Optical and Electrochemical Data of all Polymers

	UV−vis Absorption						cyclic voltammetry		
	chlorobenze solution			film			E^{ox}_{onset} (V)	E^{red}_{onset} (V)	
polymer	λ_{max} [nm]	λ_{onset} [nm]	$E_g{}^a$ [eV]	λ_{max} [nm]	λ_{onset} [nm]	$E_g{}^a$ [eV]	HOMO [eV]	LUMO [eV]	electrochemical E_g [eV]
PNDT-TT	633	890	1.39	661	900	1.38	−0.10/−4.70	−1.86/−2.94	1.76
PNDT-FTT	599	840	1.48	638	870	1.43	0.20/−5.00	−1.69/− 3.11	1.89
PQDT-TT	619	865	1.43	635	890	1.39	0.19/−4.99	−1.86/−2.94	2.05
PQDT-FTT	655	870	1.43	650	880	1.41	0.36/−5.16	−1.65/−3.15	2.01
PBnDT-TT	655	820	1.51	650	865	1.43	0.32/−5.12	−1.85/−2.95	2.16
PBnDT-FTT	633	790	1.57	638	860	1.44	0.51/−5.31	−1.83/−2.97	2.34

[a] Calculated from the intersection of the tangent on the low energetic edge of the absorption spectrum with the baseline.

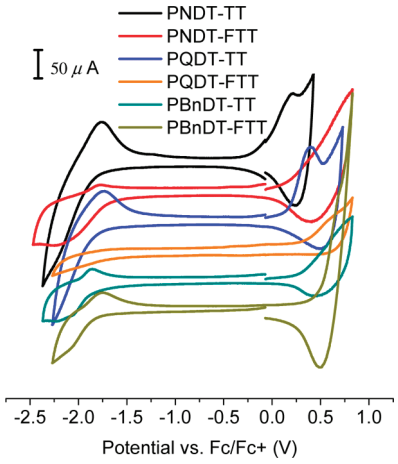

Figure 4. Cyclic voltammograms of the oxidation and reduction behavior of thin films of PNDT-TT, PNDT-FTT, PQDT-TT, PQDT-FTT, PBnDT-TT, and PBnDT-FTT.

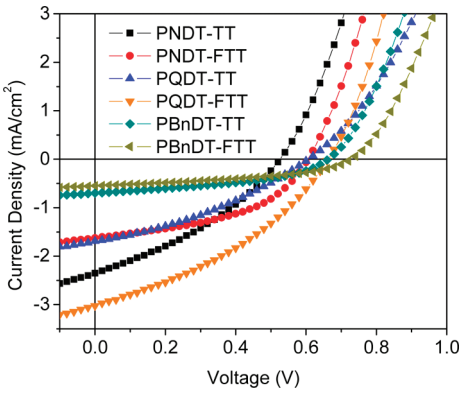

Figure 5. Characteristic $J-V$ curves of the optimized devices of polymer-based BHJ solar cells under 1 Sun condition (100 mW/cm^2).

decreases the HOMO energy level of all three TT based polymers by ∼0.2 eV (0.17−0.3 eV), consistent with the previous report.[22] This represents another means of further fine-tuning the HOMO energy level in these polymers incorporating prequinoid structures.

Photovoltaic Properties. The photovoltaic properties of these six polymers were probed via BHJ PV devices with a typical configuration of ITO/PEDOT:PSS(40 nm)/polymer:$PC_{61}BM$/Ca(40 nm)/Al(70 nm). All PV devices were tested under simulated AM1.5G illumination (100 mW/cm^2). Typical current density−voltage ($J-V$) characteristics are shown in Figure 5 and summarized in Table 3. The power conversion efficiencies were all less than 1%, including those of PBnDT-TT- and PBnDT-FTT-based devices as the "control". As expected, the V_{oc} increased consistently with the decreasing HOMO level, comparable to those achieved by Liang et al.[21,22] However, the highest J_{sc} achieved was only 3 mA/cm^2 in the case of PQDT-FTT, far less than the over 10 mA/cm^2 achieved with PBnDT-TT and PBnDT-FTT polymers in the literature.[21,22] Polymers of insufficient molecular weight can severely limit the current in BHJ devices,[29−34] which could play an important role in the case of NDT- and QDT-based polymers with relatively low molecular weight. However, the molecular weight argument would not apply to the PBnDT-TT and PBnDT-FTT polymers, which have high molecular weight but yielded even lower currents of 0.70 and 0.55 mA/cm^2 in corresponding BHJ devices, respectively. It must be noted, however, that the PBnDT-TT- and PBnDT-FTT-based polymers made by Liang et al.[21,22] had side chains much shorter than those used in this study. It is possible that this combination of monomers is particularly sensitive to longer side chains, which can reduce the ability of charges to hop between polymer chains and transfer current.[26]

Table 3. PV Performances of All Polymers

polymer	polymer: PCBM	thickness (nm)	J_{sc} (mA/cm^2)	V_{oc} (V)	FF	η (%)
PNDT-TT	1:1	95	2.37	0.53	0.34	0.43
PNDT-FTT	1:1	70	1.58	0.61	0.48	0.46
PQDT-TT	1:1	70	1.59	0.61	0.34	0.33
PQDT-FTT	1:1	80	3.00	0.67	0.36	0.73
PBnDT-TT	1:1	90	0.70	0.66	0.43	0.19
PBnDT-FTT	1:1	100	0.55	0.73	0.44	0.18

Table 4. Mobility of Polymers under SCLC Condition

	polymer:PCBM (1:1)		polymer only	
polymer	thickness (nm)	mobility (cm^2/(V s))	thickness (nm)	mobility (cm^2/(V·s))
PNDT-TT	75	7.71×10^{-6}	50	5.12×10^{-6}
PNDT-FTT	85	3.20×10^{-5}	50	6.24×10^{-6}
PQDT-TT	75	1.55×10^{-5}	60	5.15×10^{-6}
PQDT-FTT	80	5.84×10^{-6}	50	2.66×10^{-6}
PBnDT-TT	70	1.40×10^{-5}	60	6.44×10^{-7}
PBnDT-FTT	70	9.68×10^{-6}	50	7.22×10^{-6}

The hole mobility of these polymers and their BHJ blends measured by space charge limited current (SCLC) offers additional evidence to explain the observed low J_{sc} (Table 4). In general, the hole mobilities of all six polymers in their BHJ blends are very low ($10^{-5}-10^{-6}$ cm^2/(V·s)) compared to 10^{-4} cm^2/(V·s) for the PTB series reported by Liang et al.[22] The bulkier side chains on the BnDT polymers in this study (C9C4 vs C8) may increase the steric hindrance and interfere with interchain packing which would lower the hole mobility. The low hole mobilities in the NDT and QDT polymers, however, cannot be explained by the presence of bulky side chains, since these monomers also incorporated side chains of only eight carbons each. As mentioned previously, molecular weight issues may also be causing this poor hole mobility.

Conclusion

We show that the incorporation of the prequinoid unit, thienothiophene (TT), as one comonomer into the conjugated backbone leads to small-band-gap polymers, regardless of the other comonomer (e.g., NDT, QDT, or BnDT). However, the energy levels of these polymers can still be tuned by varying the electron-donating ability of the comonomer to the TT unit. Adding substituents such as fluorine to the conjugated backbone offers additional control over the energy levels with low-band-gap character conserved. Therefore, the open-circuit voltage of related BHJ devices increases consistently with decreasing HOMO levels of individual polymers.

However, the short-circuit currents of all six studied polymer-based BHJ devices are significantly lower than the values reported for similar polymer-based devices, even in the case of PBnDT-TT and PBnDT-FTT which have the identical backbone to the PTB series as reported.[21,22] The noticeably longer side chains on PBnDT series polymers in our study could account for the lower-than-expected J_{sc}, while the unsatisfactory molecular weight in the NDT- and QDT-based polymers could deter the achieving of a high current. Our study provides another example showing that the materials optimization to achieve high-efficiency polymer solar cells is a convoluted process; side chain length (and shape) and molecular weight, in addition to band gap and energy levels, all need to be carefully evaluated.

Experimental Section

Reagents and Instrumentation. All reagents and chemicals were purchased from commercial sources (Aldrich, Acros, Strem, Fluka) and used without further purification unless stated otherwise. Reagent grade solvents were dried when necessary and purified by distillation. Microwave-assisted polymerizations were conducted in a CEM Discover Benchmate microwave reactor. Gel permeation chromatography (GPC) measurements were performed on a Waters 2695 separations module apparatus with a differential refractive index detector, employing tetrahydrofuran (THF) as the eluent. The obtained molecular weight is relative to the polystyrene standard. UV−vis absorption spectra were obtained by a Shimadzu UV-2401PC spectrophotometer. For the measurements of thin films, polymers were spun-coated onto precleaned glass slides from 10 mg/mL polymer solutions in *o*-dichlorobenzene. The thicknesses of films were recorded by a profilometer (Alpha-Step 200, Tencor Instruments). An Asylum Research MFP3D atomic force microscope was used for taking AFM images. ^{1}H nuclear magnetic resonance (NMR) measurements were recorded with a Bruker 400 MHz DRX spectrometer. Chemical shifts were expressed in parts per million (ppm), and splitting patterns are designated as s (singlet), d (doublet), m (multiplet), and br (broad). Coupling constants J are reported in hertz (Hz).

Synthesis of Polymers. *PNDT-FTT*. To a 10 mL microwave-pressurized vial equipped with a stir bar, distannylated naphtho-[2,1-*b*:3,4-*b*′]dithiophene (NDT), (119 mg, 0.15 mmol), octyl 4,6-dibromo-3-fluorothieno[3,4-*b*]thiophene-2-carboxylate (FTT), (71 mg, 0.15 mmol), $Pd_2(dba)_3$ (5%) and P(o-tol)$_3$ (40%) were added. The tube was then sealed and evacuated and refilled with argon for three cycles and 0.5 mL chlorobenzene was added inside a glovebox. The reaction tube was placed in a microwave reactor and heated to 150 °C under 300 W microwave for 20 min. After cooling to room temperature, the organic solution was added dropwise to 200 mL of methanol to obtain precipitate, which was collected by filtration and washed with methanol and dried. The crude polymer was then extracted subsequently with methanol, ethyl acetate, hexane, and $CHCl_3$ in a Soxhlet's extractor. The residue after extracting with $CHCl_3$ was collected by precipitation into methanol and dried under reduced pressure to give the polymer PNDT-FTT (67 mg, 58%) as a dark blue solid.

Polymers PQDT-TT, PQDT-FTT, and PBnDT-FTT were synthesized with respective monomers according to the same procedure as PNDT-FTT. PNDT-TT was synthesized according to the same procedure as PNDT-FTT, but a THF fraction was obtained before the final $CHCl_3$ fraction and was combined with the final product.

PBnDT-TT. To a flame-dried 25 mL two-neck round-bottom flask with stir bar and reflux condenser was added 2-ethylhexyl 4,6-dibromothieno[3,4-*b*]thiophene-2-carboxylate (TT) (68 mg, 0.15 mmol) with 10 mL of toluene. Under positive argon pressure, 4,8-bis(3-butylnonyl)benzo[1,2-*b*:4,5-*b*′]dithiophene (BnDT) (135 mg, 0.15 mmol), P(*o*-tol)$_3$ (40%), and $Pd_2(dba)_3$ (5%) were then added in rapid succession. The polymerization was carried out at 120 °C for 24 h under argon protection. After cooling to room temperature, the organic solution was concentrated under reduced pressure and was added dropwise to 200 mL of methanol to obtain precipitate, which was collected by filtration and washed with methanol and dried. The crude polymer was dissolved in $CHCl_3$, filtered through Celite to remove the metal catalyst, and then precipitated into ethyl acetate and dried under reduced pressure to give the polymer PBnDT-TT (67 mg, 64%) as a dark blue solid.

The polymerization yields and ^{1}HNMR characterization data obtained for all six polymers are listed below:

PNDT-TT: (51% yield). ^{1}H NMR (400 MHz, $CDCl_2CDCl_2$, 400 K): δ 0.75−1.15 (18H, br), 1.21−1.75 (24H, br), 1.76−2.13 (3H, br), 2.93 (4H, br), 4.40 (2H, br), 8.14 (5H, br).

PNDT-FTT: (58% yield). ^{1}H NMR (400 MHz, $CDCl_2$-$CDCl_2$, 400 K): δ 0.67−1.22 (15H, br), 1.22−1.80 (28H, br), 1.80−2.15 (4H, br), 2.65−3.10 (4H, br), 4.28−4.62 (2H, br), 7.52−8.43 (4H, br).

PQDT-TT: (29% yield). ^{1}H NMR (400 MHz, $CDCl_2CDCl_2$, 400 K): δ 0.65−1.23 (18H, br), 1.23−2.22 (24H, br), 2.22−2.43 (3H, br), 3.14 (4H, br), 4.44 (2H, br), 7.76−8.62 (3H, br).

PQDT-FTT: (68% yield). ^{1}H NMR (400 MHz, $CDCl_2$-$CDCl_2$, 400 K): δ 0.78−1.20 (27H, br), 1.21−2.05 (57H, br), 2.11−2.45 (2H, br), 3.09 (4H, br), 4.45 (2H, br), 8.33 (2H, br).

PBnDT-TT: (64% yield). ^{1}H NMR (400 MHz, $CDCl_2$-$CDCl_2$, 400 K): δ 0.87−1.30 (18H, br), 1.31−1.82 (42H, br), 1.82−2.15 (5H, br), 2.65−3.37 (4H, br), 4.28−4.68 (2H, br), 7.20−8.30 (3H, br).

PBnDT-FTT: (23% yield). ^{1}H NMR (400 MHz, $CDCl_2$-$CDCl_2$, 400 K): δ 0.85−1.23 (15H, br), 1.30−1.73 (53H, br), 1.79−2.19 (4H, br), 2.82−3.37 (2H, br), 4.48 (2H, br), 7.05−8.00 (2H, br).

Electrochemistry. Cyclic voltammetry measurements were carried out using a Bioanalytical Systems (BAS) Epsilon potentiostat equipped with a standard three-electrode configuration. Typically, a three-electrode cell equipped with a glass carbon working electrode, a $Ag/AgNO_3$ (0.01 M in anhydrous acetonitrile) reference electrode, and a Pt wire counter electrode was employed. The measurements were done in anhydrous acetonitrile with tetrabutylammonium hexafluorophosphate (0.1 M) as the supporting electrolyte under an argon atmosphere at a scan rate of 100 mV/s. Polymer films were drop-cast onto the glassy carbon working electrode from a 2.5 mg/mL chloroform solution and dried under house nitrogen stream prior to measurements. The electrochemical onsets were determined at the position where the current starts to differ from the baseline. The potential of $Ag/AgNO_3$ reference electrode was internally calibrated by using the ferrocene/ferrocenium redox couple (Fc/Fc^+), which has a known reduction potential of −4.8 eV. The highest occupied molecular orbital (HOMO) and lowest unoccupied molecular orbital (LUMO) energy levels of copolymers were calculated from the onset oxidation potentials (E^{ox}_{onset}) and onset reductive potentials (E^{red}_{onset}), respectively, according to eqs 1 and 2.

$$\mathrm{HOMO} = -(E^{ox}_{onset} + 4.8)\ (\mathrm{eV}) \quad (1)$$

$$\mathrm{LUMO} = -(E^{red}_{onset} + 4.8)\ (\mathrm{eV}) \quad (2)$$

Polymer Solar Cell Fabrication and Testing. Glass substrates coated with patterned indium-doped tin oxide (ITO) were purchased from Thin Film Devices, Inc. The 150 nm sputtered ITO pattern had a resistivity of 15Ω/□. Prior to use, the substrates were ultrasonicated for 20 min in acetone followed by deionized water and then 2-propanol. The substrates were dried under a stream of nitrogen and subjected to the treatment of UV-ozone over 30 min. A filtered dispersion of PEDOT:PSS in water (Baytron PH500) was then spun-cast onto clean ITO substrates at 4000 rpm for 60 s and then baked at 140 °C for 10 min to give a thin film with a thickness of 40 nm. A blend of polymer and [6,6]-phenyl-C_{61}-butyric acid methyl ester (PCBM) (1:1 w/w, 10 mg/mL for polymers) was dissolved in *o*-dichlorobenzene with heating at 100 °C for 6 h. All the solutions were spun-cast at 1100 rpm for 60 s onto the PEDOT:PSS layer. The substrates were then dried at room temperature in the glovebox under a nitrogen atmosphere for 12 h. The devices were finished for measurement after thermal deposition of a 40 nm film of calcium and a 70 nm aluminum film as the cathode at a pressure of $\sim 1 \times 10^{-6}$ mbar. There are 8 devices per substrate, with an active area of 12 mm^2 per device. Device characterization was carried out under AM 1.5G irradiation with the intensity of 100 mW/cm^2 (Oriel 91160, 300 W) calibrated by a NREL certified standard silicon cell. Current versus potential ($I-V$) curves were recorded with a Keithley 2400 digital source meter. EQE were detected under monochromatic illumination (Oriel Cornerstone 260 1/4 m monochromator equipped with Oriel 70613NS QTH lamp), and the calibration of the incident light was performed with a monocrystalline silicon diode. All fabrication steps after adding the PEDOT:PSS layer onto ITO substrate, and characterizations were performed in gloveboxes under a nitrogen atmosphere.

For mobility measurements, the hole-only devices in a configuration of ITO/PEDOT:PSS (40 nm)/copolymer-PCBM/Pd (50 nm) were fabricated. The experimental dark current densities J of polymer:PCBM blends were measured when applied with voltage from 0 to 6 V. The applied voltage V was corrected from the built-in voltage V_{bi} which was taken as a compensation voltage $V_{bi} = V_{oc} + 0.05$ V and the voltage drop V_{rs} across the indium tin oxide/poly(3,4-ethylene-dioxythiophene):poly(styrenesulfonic acid) (ITO/PEDOT:PSS) series resistance and contact resistance, which is found to be around 35 Ω from a reference device without the polymer layer. From the plots of $J^{0.5}$ vs V, hole mobilities of copolymers can be deduced from

$$J = \frac{9}{8}\varepsilon_r \varepsilon_0 \mu_h \frac{V^2}{L^3}$$

where ε_0 is the permittivity of free space, ε_r is the dielectric constant of the polymer which is assumed to be around 3 for the conjugated polymers, μ_h is the hole mobility, V is the voltage drop across the device, and L is the film thickness of active layer.

Acknowledgment. This work was supported by the University of North Carolina at Chapel Hill, a DuPont Young Professor Award, Office of Naval Research (Grant N000140911016), and NSF CAREER Award (DMR-0954280). Nabil Kleinhenz thanks the Ernest Eliel Undergraduate Scholarship awarded by the North Carolina Section of the ACS (NC ACS) and a Summer Undergraduate Research Fellowship administered by UNC Chapel Hill.

Supporting Information Available: NMR spectra of all polymers, UV−vis of polymer/PCBM blend in films, AFM images of thin films of blends for all devices, and characteristic J-V curve and PV performance of poly(3-hexylthiophene) (P3HT) based reference device. This material is available free of charge via the Internet at http://pubs.acs.org.

References and Notes

(1) Dennler, G.; Scharber, M. C.; Brabec, C. J. *Adv. Mater.* **2009**, *21*, 1323.
(2) Cheng, Y.-J.; Yang, S.-H.; Hsu, C.-S. *Chem. Rev.* **2009**, *109*, 5868.
(3) Xiao, S.; Price, S. C.; Zhou, H.; You, W. *ACS Symp. Ser.* **2010**, *1034*, 71.
(4) Liang, Y.; Xu, Z.; Xia, J.; Tsai, S.-T.; Wu, Y.; Li, G.; Ray, C.; Yu, L. *Adv. Mater.* **2010**, *22*, E135.
(5) Chen, H.-Y.; Hou, J.; Zhang, S.; Liang, Y.; Yang, G.; Yang, Y.; Yu, L.; Wu, Y.; Li, G. *Nature Photonics* **2009**, *3*, 649.
(6) Havinga, E. E.; Tenhoeve, W.; Wynberg, H. *Synth. Met.* **1993**, *55−57*, 299.
(7) Ajayaghosh, A. *Chem. Soc. Rev.* **2003**, *32*, 181.
(8) Jenekhe, S. A.; Lu, L.; Alam, M. M. *Macromolecules* **2001**, *34*, 7315.
(9) Zhu, Y.; Champion, R. D.; Jenekhe, S. A. *Macromolecules* **2006**, *39*, 8712.
(10) Xiao, S.; Stuart, A. C.; Liu, S.; You, W. *ACS Appl. Mater. Interfaces* **2009**, *1*, 1613.
(11) Xiao, S.; Stuart, A. C.; Liu, S.; Zhou, H.; You, W. *Adv. Funct. Mater.* **2010**, *20*, 635.
(12) Brédas, J.-L.; Norton, J. E.; Cornil, J.; Coropceanu, V. *Acc. Chem. Res.* **2009**, *42*, 1691.
(13) Wudl, F.; Kobayashi, M.; Heeger, A. J. *J. Org. Chem.* **1984**, *49*, 3382.
(14) Pomerantz, M.; Chalonergill, B.; Harding, L. O.; Tseng, J. J.; Pomerantz, W. J. *J. Chem. Soc., Chem. Commun.* **1992**, 1672.
(15) Hong, S. Y.; Marynick, D. S. *Macromolecules* **1992**, *25*, 4652.
(16) Sotzing, G. A.; Lee, K. H. *Macromolecules* **2002**, *35*, 7281.
(17) Kroon, R.; Lenes, M.; Hummelen, J. C.; Blom, P. W. M.; de Boer, B. *Polym. Rev.* **2008**, *48*, 531.
(18) Qin, Y.; Kim, J. Y.; Frisbie, C. D.; Hillmyer, M. A. *Macromolecules* **2008**, *41*, 5563.
(19) Zhou, H.; Yang, L.; Stoneking, S.; You, W. *ACS Appl. Mater. Interfaces* **2010**, *2*, 1377.
(20) Zhou, H.; Yang, L.; Price, S. C.; Knight, K. J.; You, W. *Angew. Chem., Int. Ed.* **2010**, *49*, 7992.
(21) Liang, Y.; Wu, Y.; Feng, D.; Tsai, S.-T.; Son, H.-J.; Li, G.; Yu, L. *J. Am. Chem. Soc.* **2009**, *131*, 56.
(22) Liang, Y.; Feng, D.; Wu, Y.; Tsai, S.-T.; Li, G.; Ray, C.; Yu, L. *J. Am. Chem. Soc.* **2009**, *131*, 7792.
(23) Xiao, S.; Zhou, H.; You, W. *Macromolecules* **2008**, *41*, 5688.
(24) Price, S. C.; Stuart, A. C.; You, W. *Macromolecules* **2010**, *43*, 797.
(25) Price, S. C.; Stuart, A. C.; You, W. *Macromolecules* **2010**, *43*, 4609.
(26) Yang, L.; Zhou, H.; You, W. *J. Phys. Chem. C* **2010**, *114*, 16793.
(27) Rieger, R.; Beckmann, D.; Mavrinskiy, A.; Kastler, M.; Müllen, K. *Chem. Mater.* **2010**, *22*, 5314.
(28) He, M.; Li, J.; Tandia, A.; Sorensen, M.; Zhang, F.; Fong, H. H.; Pozdin, V. A.; Smilgies, D.-M.; Malliaras, G. G. *Chem. Mater.* **2010**, *22*, 2770.
(29) Schilinsky, P.; Asawapirom, U.; Scherf, U.; Biele, M.; Brabec, C. J. *Chem. Mater.* **2005**, *17*, 2175.
(30) Morana, M.; Wegscheider, M.; Bonanni, A.; Kopidakis, N.; Shaheen, S.; Scharber, M.; Zhu, Z.; Waller, D.; Gaudiana, R.; Brabec, C. *Adv. Funct. Mater.* **2008**, *18*, 1757.
(31) Ballantyne, A. M.; Chen, L.; Dane, J.; Hammant, T.; Braun, F. M.; Heeney, M.; Duffy, W.; McCulloch, I.; Bradley, D. D. C.; Nelson, J. *Adv. Funct. Mater.* **2008**, *18*, 2373.
(32) Ma, W.; Kim, J. Y.; Lee, K.; Heeger, A. J. *Macromol. Rapid Commun.* **2007**, *28*, 1776.
(33) Bijleveld, J. C.; Zoombelt, A. P.; Mathijssen, S. G. J.; Wienk, M. M.; Turbiez, M.; de Leeuw, D. M.; Janssen, R. A. J. *J. Am. Chem. Soc.* **2009**, *131*, 16616.
(34) Zhou, H.; Yang, L.; Xiao, S.; Liu, S.; You, W. *Macromolecules* **2010**, *43*, 811.